Turbulent flow in pulsed extraction columns with internals of discs and rings:Turbulent kinetic energy and its dissipation rate during the pulsation

George Angelov, Christophe Gourdon

▶ **To cite this version:**

George Angelov, Christophe Gourdon. Turbulent flow in pulsed extraction columns with internals of discs and rings:Turbulent kinetic energy and its dissipation rate during the pulsation. Chemical Engineering and Processing: Process Intensification, 2009, vol. 48 (n° 2), pp. 592-599. 10.1016/J.CEP.2008.07.002 . hal-03562762

HAL Id: hal-03562762
https://hal.science/hal-03562762

Submitted on 9 Feb 2022

HAL is a multi-disciplinary open access archive for the deposit and dissemination of scientific research documents, whether they are published or not. The documents may come from teaching and research institutions in France or abroad, or from public or private research centers.

L'archive ouverte pluridisciplinaire **HAL**, est destinée au dépôt et à la diffusion de documents scientifiques de niveau recherche, publiés ou non, émanant des établissements d'enseignement et de recherche français ou étrangers, des laboratoires publics ou privés.

Open Archive Toulouse Archive Ouverte (OATAO)
OATAO is an open access repository that collects the work of Toulouse researchers and makes it freely available over the web where possible.

This is an author-deposited version published in: http://oatao.univ-toulouse.fr/
Eprints ID: 5940

To link to this article: DOI:10.1016/J.CEP.2008.07.002
URL: http://dx.doi.org/10.1016/J.CEP.2008.07.002

To cite this version: Angelov, George and Gourdon, Christophe (2009) Turbulent flow in pulsed extraction columns with internals of discs and rings: Turbulent kinetic energy and its dissipation rate during the pulsation. *Chemical Engineering and Processing : Process Intensification*, vol. 48 (n°2). pp. 592-599. ISSN 0255-2701

Any correspondence concerning this service should be sent to the repository administrator: staff-oatao@listes.diff.inp-toulouse.fr

Turbulent flow in pulsed extraction columns with internals of discs and rings: Turbulent kinetic energy and its dissipation rate during the pulsation

G. Angelov[a,*], C. Gourdon[b]

[a] Institute of Chemical Engineering, Bulgarian Academy of Sciences, Acad. Bonchev Street, Block 103, 1113 Sofia, Bulgaria
[b] Ecole Nationale Supérieure des Ingénieurs en Arts Chimiques et Technologiques, Institut National Polytechnique, 31000 Toulouse, France

A B S T R A C T

Turbulent energy parameters of single-phase pulsed flow in an extraction column with internals of immobile discs and rings (doughnuts) are studied. Simulation results are obtained by resolution of Reynolds equations coupled with k–ε model of turbulence. As far as pulsed flow is concerned, the evolution of space distribution of turbulent kinetic energy k and its dissipation rate ε during the pulsation is thoroughly studied. It is observed that the energy distribution on a contact stage changes periodically from rather homogeneous to highly inhomogeneous depending on instantaneous flow velocity. Significant difference between maximal and mean energy parameters is observed. It is supposed that the discrepancy between simulation and experimental results for the size of drops formed in the turbulent field might be attributed to mean energy presentation that smoothes the peak effects of a pulsed flow. Spatial zones and time intervals of high-turbulent kinetic energy are delimited presuming their dominant role for accurate foreseeing of size of drops in this type of equipment. It is shown that an "effective" energy level should be determined by selection over the high-energy time periods and zones in order to compensate the smoothing effect of mean energy level.

The results obtained are useful for the calculation of drop size based on energy level at the stage, which is necessary for the determination of parameters of practical interest such as drop residence time and interphase mass transfer surface.

1. Introduction

Solvent extraction is a basic mass transfer process largely used in the chemical technology [1]. External energy is often applied to the contact apparatuses in order to improve the phase contact. The performance of extraction columns is often ameliorated by use of pulsations [2–4]. They modify the apparatus hydrodynamics by inducing turbulence to the flow thus improving the interphase contact and intensifying the mass transfer. So, the comprehension of process intensification mechanisms requires knowledge about the state of turbulence. The latter is characterized by a number of parameters, the main among them being the turbulent kinetic energy k and its dissipation rate ε [5,6].

Regarding pulsed columns, important change of flow behavior is observed during a periodic pulsation. The flow alternates twice its direction (upward and downward) taking velocity from zero to a maximal value. Correspondingly to flow velocity changes, variation of turbulent energy level in the course of time is to be expected. Previous hydrodynamic investigations on the extraction equipment studied here (column with internals of discs and rings) focused towards the mean turbulent flow parameters [7–11]. There are indications that important process parameters, being determined through the mean values of turbulent energy terms, are incorrectly estimated. For example, the dispersed phase drop size is overestimated [9,11], which is a sign of underestimated flow energy. A possible explanation is that the mean energy parameters do not represent well enough the particular periodic character of a pulsed flow. More knowledge about the evolution of turbulent energy field during the pulsation will be helpful for understanding the role of pulsations on the hydrodynamics of column apparatuses. The task of this paper is to reveal in details the instantaneous space distribution of important turbulent flow characteristics (k and ε) and its time evolution during the pulsation cycle in order to examine the role of high-energy levels of a pulsation in drop splitting and interphase surface formation processes as compared to that of mean energy level.

* Corresponding author.
E-mail address: gang@bas.bg (G. Angelov).

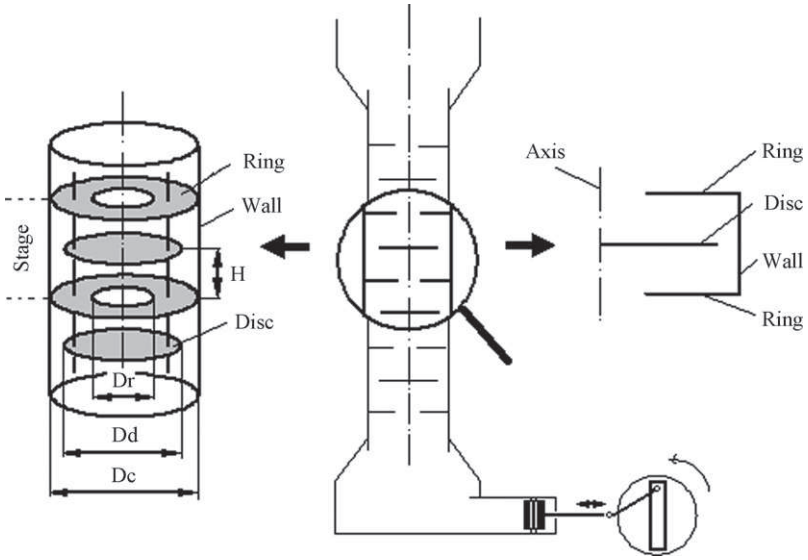

Fig. 1. Apparatus scheme: left, plate geometry; center, a sketch of the column and right, stage simulation domain.

2. Apparatus description

The apparatus (Fig. 1) has cylinder body divided in stages by alternating internals of immobile discs and rings (rings are called also doughnuts) placed equidistantly at a distance H. A stage is limited between two rings with a disc between them, dividing the stage in two compartments—lower and upper. The plates form two types of passages for the flow: central aperture of the ring (with diameter D_r) and peripheral annular aperture between the disc and column wall. Both of them have equal open area. The disc (with diameter D_d) is larger than the ring aperture (D_r) in order to hamper a direct axial passage through the column. In normal operation, two immiscible liquids with different density flow counter-currently through the apparatus. One of them is in large quantity (continuous phase), while the other, being in minor quantity (several percents), is dispersed as drops. A mechanical device creates periodical pulsations.

The geometric dimensions of the experimental column are as follows:

- Column diameter, $D_c = 0.29$ m
- Height of the body filled with disk-ring internals, 2.40 m
- Total number of internals, 51
- Number of constructive stages, 25
- Distance between two adjacent internals, $H = 0.045$ m
- Disc diameter, $D_d = 0.254$ m
- Diameter of ring aperture, $D_r = 0.14$ m
- Free area of the internals, $F = 23\%$

3. Mathematical description

As far as we study the turbulent energy field induced to the continuous phase by pulsations, we consider here one-phase incompressible Newtonian liquid (a typical continuous phase of an extraction system is usually an aqueous solution). It is assumed that a repeated space structure creates spatial periodicity, and the periodic sinusoidal pulsation creates time periodicity. Axisymmetrical flow is presumed because of the arrangement of all constructive elements in a cylindrical shell symmetrically to the apparatus central axis.

The assumption for space periodicity and axial symmetry has been confirmed experimentally [7,12], and one can regard the situation in a single stage as representative for the whole column. Oh [13] has measured rather small tangential component of velocity vector thus making possible to consider two-dimensional flow with radial and axial velocity components. Because of axial symmetry, the stage presentation may be restricted to a vertical stage cross-section limited by two rings above and below, by the column axis at left and by the column wall at right (see Fig. 1—right).

The flow velocity can be split in two components, a permanent (U_o) and a periodical one $U_p(t)$. The first is determined by the column throughput (quantity of flow passing through the column at a time), while the periodical component is due to pulsation.

As it is found for pulsed columns, when $U_p(t)$ is significantly larger than U_o, the permanent velocity does not influence the drop size [14]. In real industrial operation the pulsation velocity is dominant. The ratio $U_p(t)/U_o$ falls in the range 50–90, so the permanent velocity can be neglected [15]. Thus the instantaneous flow velocity may be approximately expressed by its periodical component. In case of a piston pulsing device it is sinusoidal function of time expressed by the relation:

$$U_p(t) = \pi A f \cos 2\pi f t \tag{1}$$

where A and f are the pulsation amplitude and frequency.

Re number for the flow is defined with respect to its mean superficial velocity U_m obtained by integrating the instantaneous velocity $U_p(t)$ over a pulsation period:

$$Re = \frac{U_m D_c}{\nu} = \frac{2AfD_c}{\nu} \tag{2}$$

where ν is kinematic viscosity.

The interval of Re values studied here is 5000–15,000. It has been chosen because of the experimental estimation for this space configuration that at Re higher than 5000 the flow completely loses its laminar pattern and becomes distinctly turbulent [13]. This region coincides with operational regimes of real equipment, and drop size experimental data are available, too [16].

For the description of turbulent flow regimes we have used statistically averaged equations of Navier–Stokes (Reynolds equations) applied for the case of incompressible fluid with constant density and viscosity [6]. The turbulent stresses appearing in Reynolds equations should be determined by a turbulence model. Its choice is based on the following reasons.

Studies on pulsed flow in pipes have revealed that one- and two-equation models of turbulence based on turbulence viscosity

concept describe quite well the flow in case of frequency of mechanical pulsations significantly lower than the frequency of turbulent pulsations. Two-equation models are recommended because they define more correctly the turbulent macroscale by an additional transport equation [17].

In case of our column, a spectral analysis of turbulent pulsations has been done. For $Re = 5000–15{,}000$, the mechanical pulsation frequency is about 1 Hz while the frequency of turbulent pulsations is in the zone 10–100 Hz [13]. It is seen that the two frequencies are quite different and do not interfere. Thus the models based on turbulent viscosity concept are applicable.

The two-equation k–ε model offers an optimal combination of complexity of treatment and reliable results. It is often applied for industrial flows in relatively complex geometry giving better results than other similar models [17]. So, a reasonable choice for our study is oriented towards application of k–ε model. The corresponding equations are well known. They are given in our previous paper [7] and might be also found in [18,19].

3.1. Boundary conditions

The boundary values at the stage entry/exit have been determined experimentally by means of Laser-Doppler anemometry on a central stage of the experimental column [13,20].

Unlike the work of Bujalski et al. [21], where low-Re turbulent model is used to perform simulations at $Re = 2000$, we use k–ε model like some other authors [10,22] to perform simulations at higher Re number. It requires special formulation near the walls where viscous forces become dominant. A recommended logarithmic wall function has been used to link the bulk and wall regions [18]:

$$\frac{U(y)}{U_\tau} = \frac{1}{K} \ln\left(\frac{yU_\tau}{\nu} E\right) \tag{3}$$

where $U(y)$ is the velocity in the logarithmic junction area placed outside the viscous sublayer, U_τ is friction velocity, K is Karman constant, y is the distance from the wall and E is wall roughness parameter. At the first grid point outside the viscous sublayer the turbulence is assumed to be in local equilibrium, which yields the values of k and ε:

$$k(y) = \frac{U_\tau^3}{\sqrt{C_\mu}} \tag{4}$$

$$\varepsilon(y) = \frac{U_\tau^3}{Ky} \tag{5}$$

The solution procedure is based on the finite volumes method. The equations have been discretized over a half-stage by a regular mesh with 30 points in radial and 19 points in axial direction. Details of the numerical procedure are given in Angelov et al. [7]. As a result, local values of turbulent kinetic energy k and its dissipation rate ε have been obtained for each cell of the mesh. Tests with various mesh size have also been made. The results are found to be not so sensitive to the mesh size. For example, compared to a mesh with twice smaller step, the difference of the instantaneous values of turbulent kinetic energy is lower than 2.9% and lower than 1.6% for the mean energy values.

The dispersed phase impact on the turbulent energy field in a two-phase flow has been studied in our recent paper [23]. Its influence is not strong and is demonstrated only in the moments of pulsation velocity near to zero, when the energy level is low and the dispersed phase velocity becomes comparable to pulsation velocity. It seems that the dispersed phase impact could be neglected in the case treated here because we are interested in high-energy periods of the pulsation cycle.

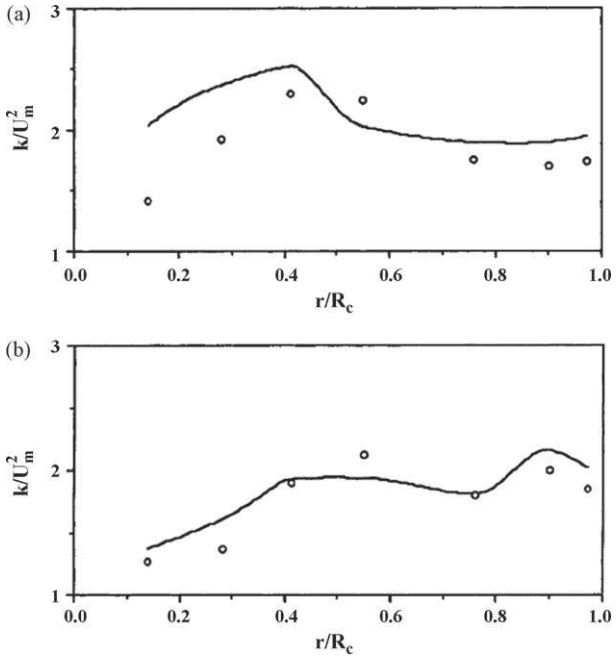

Fig. 2. Comparison of experimental (points) and simulation results (line) for turbulent kinetic energy k at the stage median level: (a) pulsation parameters; $A = 0.02$ m, $f = 0.86$ Hz, $Re = 10{,}000$ and (b) pulsation parameters; $A = 0.02$ m, $f = 1.3$ Hz, $Re = 15{,}000$.

Fig. 2 represents a confrontation of experimental and simulation results for the turbulent kinetic energy k in the column with geometrical parameters given above. The points represent results of experimental measurements of the instantaneous velocity vector with Laser-Doppler anemometry, followed by signal treatment for the determination of turbulent velocity fluctuations and turbulent kinetic energy k over a diameter of the median stage cross-section located equidistantly between a ring and a disc. Fair agreement is seen, which can be considered as a base for reliable simulations.

4. Simulation results

4.1. Turbulent kinetic energy

Fig. 3a–d illustrates the turbulent kinetic energy field over the simulation domain at $Re = 10{,}000$, a value corresponding to the middle of the studied interval ($Re = 5000–15{,}000$), and also to experimental regimes supplying data for size of drops. Each picture represents the spatial energy distribution at a different moment of the pulsation cycle. Several consecutive moments during a pulsation period are shown in order to illustrate the time evolution of energy field.

Analyzing Fig. 3, a number of zones with different energy levels can be distinguished. At the moment $t/T = 0$ (Fig. 3a), corresponding to maximum ascending velocity, zones with lowest energy (about 0.1 of the maximal energy level at the stage) are located around the rigid obstacles. Lower-energy zones (0.1–0.4 of maximal energy level) occupy a large part of the entry compartment and a smaller part of the exit compartment. Higher-energy zones are located as follows (in ascending order):

- level 0.4–0.7 of maximum: median zones between the disc and rings, zones below and above the peripheral aperture, and a zone of the ring aperture at the stage entry;
- level 0.7–0.9 of maximum: zones around the internal narrow places (the ring aperture at the stage exit and the passage between disc and wall);

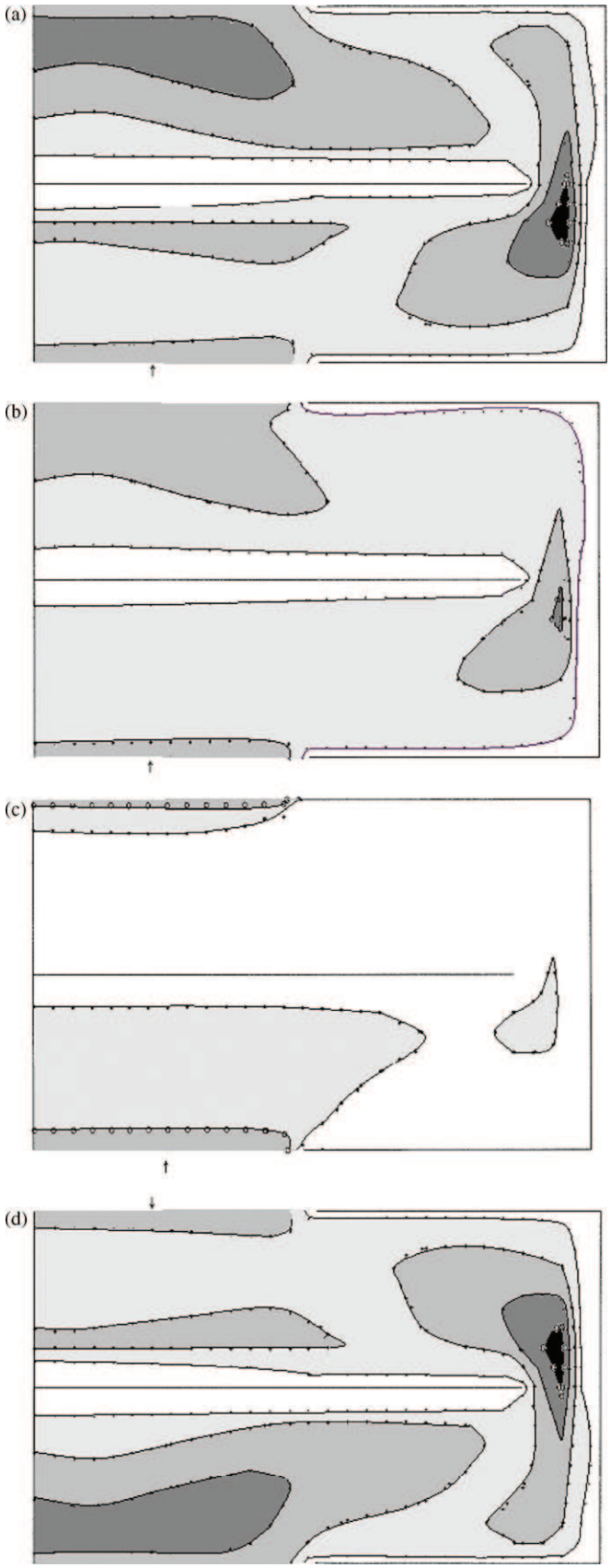

Fig. 3. Space distribution of turbulent kinetic energy k at different moments of the pulsation cycle, $Re = 10{,}000$. (a) $t/T = 0$, values of k in the different zones (m^2/s^2): (□) (0–1) × 10^{-3}; (□) (1–4) × 10^{-3}; (■) (4–7) × 10^{-3}; (■) (7–9.5) × 10^{-3} and (■) (0.95–1.11) × 10^{-2} . (b) $t/T = 0.10$, values of k (m^2/s^2): (□) (0–1) × 10^{-3}; (□) (1–4) × 10^{-3}; (■) (4–7) × 10^{-3} and (■) (7–7.4) × 10^{-3}. (c) $t/T = 0.20$, values of k (m^2/s^2): (□) (0–1) × 10^{-3}; (□) (1–2) × 10^{-3} and (■) (2–2.25) × 10^{-3}. (d) $t/T = 0.50$, values of k (m^2/s^2): (□) (0–1) × 10^{-3}; (□) (1–4) × 10^{-3}; (■) (4–7) × 10^{-3}; (■) (7–9.5) × 10^{-3} and (■) (0.95–1.11 × 10^{-2}.

o the highest energy zone is located in the vicinity of peripheral aperture disc-wall. The maximal value of turbulent kinetic energy is found inside this zone, approximately in the midst of peripheral aperture. In the highest energy zone, the energy value is more than 10 times larger than that in the lowest one (see Table 1).

It is easy to understand the location of high-energy zones. They are placed preferably in zones where the internals restrict the flow passage thus provoking velocity increase. The highest energy zone is found near the peripheral passage between the disc and column wall. At this place where the velocity is abruptly changed (from zero on the wall and disc end to maximum in the passage) in a small distance equal to 1/12 of column diameter.

In a moment of lower velocity $t/T = 0.1$ (Fig. 3b), the energy level also goes down. The volume of lower-energy zones is enlarged. Although with reduced volume, the general location of higher-energy zones is kept approximately the same and the position of maximum energy remains unchanged. Referring to line 3 of Table 1, the ratio of highest and lowest levels is smaller—7.4. The maximal value of energy at this moment is 0.67 of maximum for the whole cycle.

From the beginning of the cycle till this moment, the mean energy content of the compartments is slightly different. The lower compartment, which at this time serves as flow entry has lesser mean-energy value as compared to the upper exit compartment (see Table 1).

Approaching the pulsation's dead point (Fig. 2c) the energy level steadily goes down, and lower-energy zones occupy practically the whole stage. The ratio of highest and lowest energy level becomes as low as 2 (Table 1, line 5). It is a sign of rather uniform distribution, meaning that at low velocity the internals do not create significant local turbulence. The lower (entry) compartment contains now more energy than the upper one.

Although some difference, the function of the compartments is certainly equalized because each of them periodically takes the function of the other.

After the dead point ($t/T = 0.25$), the flow changes its direction from upward to downward. Symmetrical reproduction of the picture described above has been obtained with disc being symmetry plane. The situation in lower compartment becomes identical to that in the upper one but shifted at a half period. It is illustrated by comparison of energy fields at two moments of same velocity and opposite flow direction $t/T = 0$ and 0.5 (Fig. 3a and d; Table 1, lines 1 and 6).

During the entire pulsation period, the zones with lowest energy are always located in the vicinity of rigid obstacles (wall, disc and rings). The energy level is more important within the time intervals of higher flow velocity ($t/T = 0$–0.10, 0.4–0.6 and 0.9–1). In the course of time, the compartments alternate their functions. They have identical global behavior, which is shifted at a half pulsation period. Maximal kinetic energy is attained in the peripheral passage between the disc and wall. The zones of important energy level keep approximately constant their space location at peripheral and central passages and median zones above and below the passages. This result is in agreement with a study on drop breakage in two-phase flow in the same column [16], which reports the same zones as places where drops preferably break down in smaller droplets.

Fig. 4 shows the evolution of maximal and mean (space-averaged) values of turbulent kinetic energy k at the stage in the

Table 1
Values of turbulent kinetic energy k during a pulsation cycle, $Re = 10{,}000$

t/T	k_{max} ($\times 10^2$ m^2/s^2)	k_{max} (n)/k_{max} (1)	k_{max}/k_{min}	k_{mean} ($\times 10^2$ m^2/s^2)	k_{max}/k_{mean}	k_{mean} ($\times 10^2$ m^2/s^2)	
						Lower compartment	Upper compartment
0	1.11	1	11.1	0.40	2.78	0.38	0.46
0.05	1.03	0.93	10.3	0.36	2.75	0.32	0.41
0.10	0.74	0.67	7.4	0.29	2.59	0.28	0.32
0.15	0.43	0.39	4.3	0.18	2.36	0.24	0.17
0.20	0.22	0.20	2.2	0.08	2.63	0.15	0.07
0.50	1.11	1	11.1	0.40	2.78	0.46	0.38

course of a pulsation cycle. Their time evolution follows the sinusoidal periodicity of flow velocity.

There are two maxima corresponding to maximal upward ($t/T = 0$) and maximal downward velocity ($t/T = 0.5$), while the minima correspond to the moments of alternation of flow direction ($t/T = 0.25$ and 0.75). It is seen that the maximal values of k at the peak moments $t/T = 0$ and 0.5 are more than five times higher than the corresponding values in low-velocity/low-energy intervals of the pulsation cycle. Similar is the situation with the respective mean values, which differ also about five times. An interesting observation is that in every moment of the pulsation the ratio of maximal and mean stage energy does not change significantly (value about 2.6—see Table 1). So, during the pulsation the maximal energy value changes continuously, but it is always about 2.5 times higher than the mean energy of the stage. This fact might be useful for value estimation of an unknown term when the other one is available.

4.2. Influence of Re number on the spatial distribution of turbulent kinetic energy

Fig. 5a–c illustrates the space distribution of turbulent energy in a fixed moment of the pulsation at different *Re* numbers. Two zones with highest energy for the corresponding regime are shown. The situation for other time positions in the pulse cycle is analogous.

Higher *Re* number corresponds to higher flow velocity. The rise of *Re* produces the same impact as the rise of velocity in the course of pulsation cycle. Generally, the energy level becomes higher, the high-energy zones expand in volume and keep approximately their space location at various *Re* numbers, the latter being a sign of stable hydrodynamic regime.

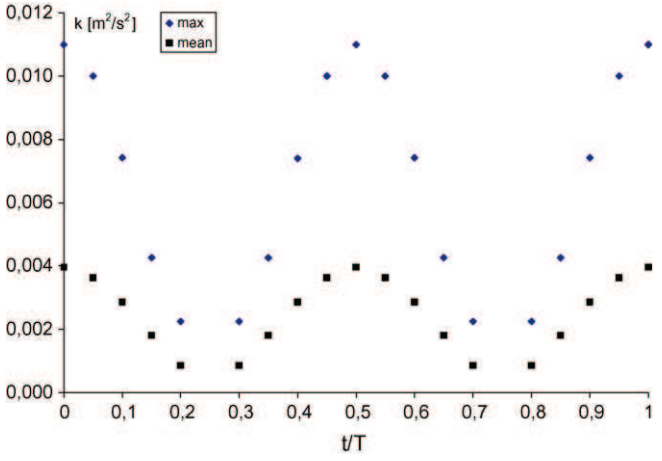

Fig. 4. Evolution of maximal and mean (space-averaged) turbulent kinetic energy k at the stage during a period of pulsation, $Re = 10{,}000$.

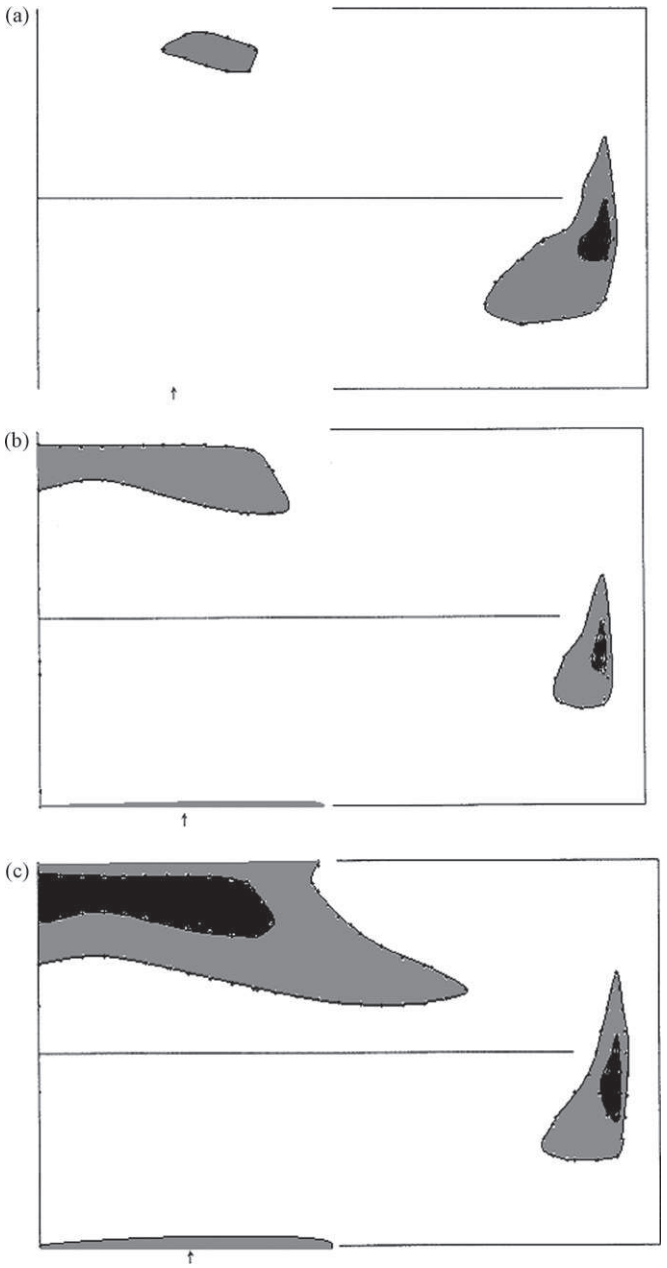

Fig. 5. Space distribution of k at various *Re* numbers, $t/T = 0.05$. (a) $Re = 5000$, values of k in the different zones (m^2/s^2): (□) (0–2) $\times 10^{-3}$; (▩) (2–3) $\times 10^{-3}$ and (■) (3–3.3) $\times 10^{-3}$. (b) $Re = 10{,}000$, values of k (m^2/s^2): (□) (0–7) $\times 10^{-3}$; (▩) (7–9.5) $\times 10^{-3}$ and (■) (0.95–1.05 $\times 10^{-2}$. (c) $Re = 15{,}000$, values of k (m^2/s^2): (□) (0–1) $\times 10^{-2}$; (▩) (1–1.5) $\times 10^{-2}$ and (■) (1.5–1.8) $\times 10^{-2}$.

4.3. Dissipation rate of the turbulent kinetic energy ε

The turbulent kinetic energy is transformed in heat by dissipation. The reason lies in the local velocity gradients that cause local stresses and deformations of the flow. According to the conventional mechanisms of energy transfer [24], the mean flow interferes only with large turbulent vortices because of the similar size of their structures. The energy received from the external source (pulsations) is spent for agitation and formation of smaller vortices. Following so-called "energy transfer cascade", the energy is transmitted from larger towards smaller vortices. Finally, reaching the scale at which viscous forces become dominant, the vortex energy dissipates being transformed into heat.

Fig. 6a and b shows the high-dissipation zones in two extreme moments $t/T = 0$ and 0.2 corresponding to high- and low-flow velocity at the stage. Pictures analogous to energy distribution are seen (compare with Fig. 3a and d). It means that the high-energy zones are also zones of high dissipation. At high-flow velocity (Fig. 6a) the main dissipation zone is the peripheral passage and the median zone in the exit compartment as well. At low velocity (Fig. 6b) the dissipation rate is significantly reduced, and entry–exit ring apertures become more important dissipation zones.

Reversing the flow direction (Fig. 6c), symmetrical changes take place as already shown and discussed when regarding the energy field.

Regarding the evolution of maximal and space-averaged values of dissipation rate ε during the pulsation cycle (Fig. 7), similar tendency is seen as in case of turbulent energy k (Fig. 4). The intervals of high- and low-dissipation rate correspond to those of the turbulent energy and are related to high- and low-velocity intervals of the pulsation cycle.

However, the energy dissipation ε is more inhomogeneous in the course of time than k. For example, regarding the values of parameters already reported for k, the ratio of maximal values of ε at the moments of high- and low-velocity is 7.4 compared to 5 for k, the same ratio for space-averaged values is 7.9 versus 5 for k, the ratio of maximal and space-averaged ε-values at the stage is relatively constant in every moment of the pulsation and is about 4.5 versus 2.6 for k.

We do not illustrate here the space distribution of dissipation at different Re numbers because of its similarity with the pictures of energy distribution shown in Fig. 5. The dissipation rate rises with Re while the space location of dissipation zones does not change significantly as it happens with stable hydrodynamic regimes.

5. Discussion

A general observation of this study on the pulsed flow regime is that large fluctuations above the mean level of turbulent kinetic energy exist in the course of a pulsation cycle. During the high-energy periods, the energy attains values much more significant than the mean values. Previous attempts to correlate the mean energy level with drop size have produced overestimated results for the drop size [9,11], which is certainly due to underestimated energy level. The presentation based on mean energy level probably smooths the peak effects of a pulsed flow. In our opinion, the high-energy levels, although existing during a part of the pulsation cycle, should have important impact on the global hydrodynamic behavior. In order to clarify this statement, we have compared simulation results for the energy at different moments of a pulsation cycle with experimental data.

For a column of same geometry, Laulan [16] has reported experimental results for maximal stable drop diameter d_s at different pulsation intensity (different Re numbers). These results can be used for estimation of the energy k_s corresponding to a given experimental value of d_s.

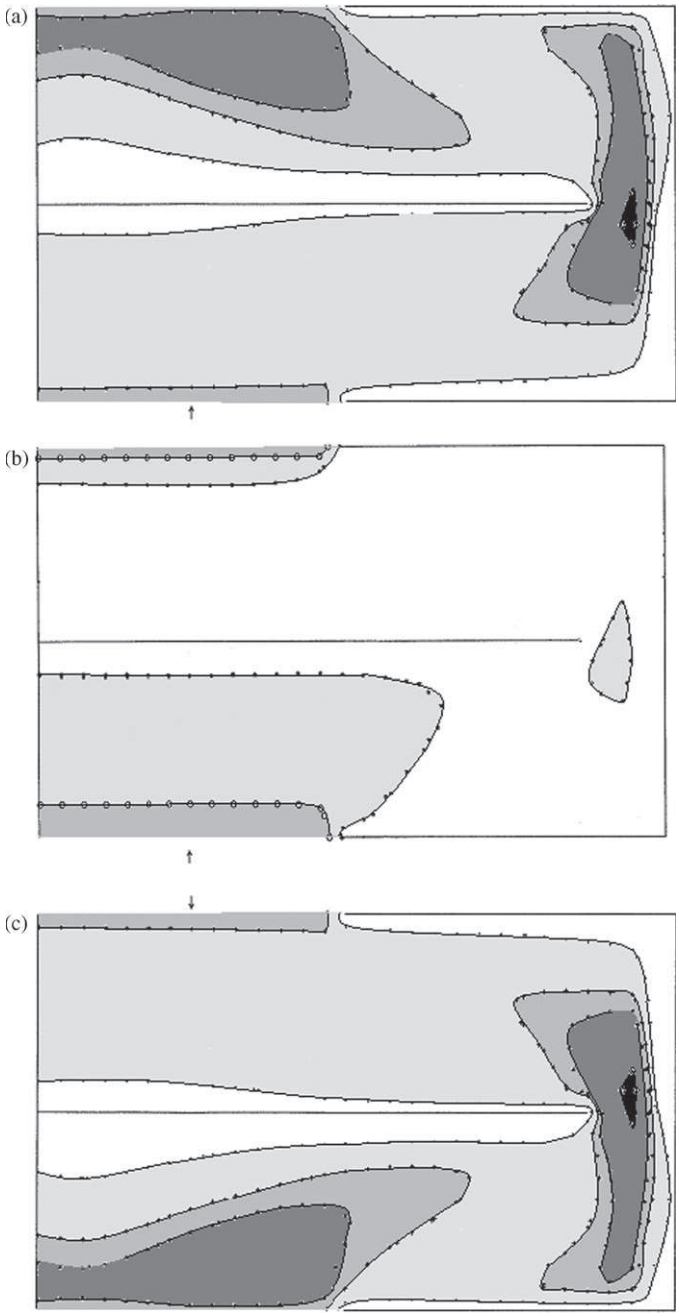

Fig. 6. Space distribution of turbulent energy dissipation rate ε at different moments of the pulsation cycle, $Re = 10{,}000$. (a) Values of ε in the different zones (m^2/s^3) at $t/T = 0$: (□) (0–5) $\times 10^{-3}$; (□) (0.5–1.5) $\times 10^{-2}$; (■) (1.5–2.10) $\times 10^{-2}$; (■) (2–5) $\times 10^{-2}$ and (■) (5–5.95) $\times 10^{-2}$. (b) Values of ε (m^2/s^3) at $t/T = 0.20$; (□) (0–5) $\times 10^{-3}$; (□) (5–7.5) $\times 10^{-3}$ and (■) (7.5–8.1) $\times 10^{-3}$. (c) Values of ε (m^2/s^3] at $t/T = 0.50$: (□) (0–5) $\times 10^{-3}$; (□) (0.5–1.5) $\times 10^{-2}$; (■) (1.5–2.10) $\times 10^{-2}$; (■) (2–5) $\times 10^{-2}$ and (■) 5–5.95 $\times 10^{-2}$

Weber number We represents the ratio of kinetic and drop surface energy:

$$We = \frac{\rho_c k d}{\sigma} \tag{6}$$

where ρ_c is continuous phase density, d is drop diameter, and σ is interfacial tension.

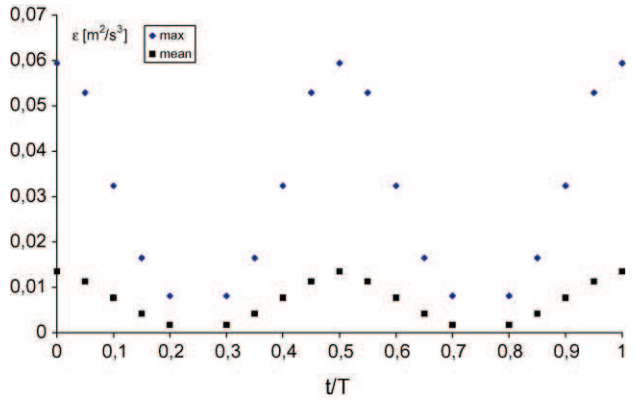

Fig. 7. Maximal and mean (space-averaged) dissipation rate ε at the stage during the pulsation, $Re = 10{,}000$.

A drop breaks in smaller drops when the kinetic energy in the continuous phase prevails over the drop surface forces. The state of equilibrium between these two forces corresponds to an equilibrium value We_e, and defines maximal stable drop diameter d_s, which does not break down at these conditions. At values higher than We_e (higher k) the drops break down until new equilibrium is attained:

$$We_e = \frac{\rho_c k_s d_s}{\sigma} \tag{7}$$

We_e can also be presented in terms of surface energy of mother and daughter drops [25]:

$$We_e = \frac{\Delta E}{\pi d^2 \sigma} \tag{8}$$

ΔE is the difference of surface energy of a mother drop splitting in n equally sized daughter drops:

$$\Delta E = \pi d^2 \sigma (n^{1/3} - 1) \tag{9}$$

From Eqs. (8) and (9) it follows:

$$We_e = n^{1/3} - 1 \tag{10}$$

Laulan [16] has observed that the breaking mother drops produce preferably two daughter drops. Then, for $n = 2$:

$$We_e = 0.26 \tag{11}$$

Now, the energy term k_s which corresponds to experimental values of d_s can be determined through Eqs. (7)–(11). The experimental conditions at which d_s has been measured are $Re = 7000$, 8700 and 10,500 (with pulsation parameters $A = 0.015$ m and $f = 0.8$, 1 and 1.2 Hz correspondingly).

Fig. 8 compares values of k_s to simulation results for the mean energy (k mean cycle—space- and time-averaged) on the stage. High discrepancy is seen making doubtful that the mean energy level represents the acting "effective" energy level. Following the results for space distribution and time evolution of energy during the pulsation cycle, two possible approaches for fixing this problem might be envisaged:

- One can search an "effective" value of k by selection over the high-energy zones. In this case their spatial limits should be postulated, and drop trajectory should be followed in order to determine the drop population exposed to high-energy level when passing through these zones. A shortcoming lies in some uncertainty in definition of zone limits, because they are changeable in the course of time. Linking of drop trajectory to zones' location needs Lagrangean-type study [26]. Additional investigation is necessary to acquire information elucidating the subject.
- The second approach is more pragmatic. If suppose that the high-energy intervals of the pulsation are responsible for drop breakage processes, then the "effective" energy value should be selected over these intervals.

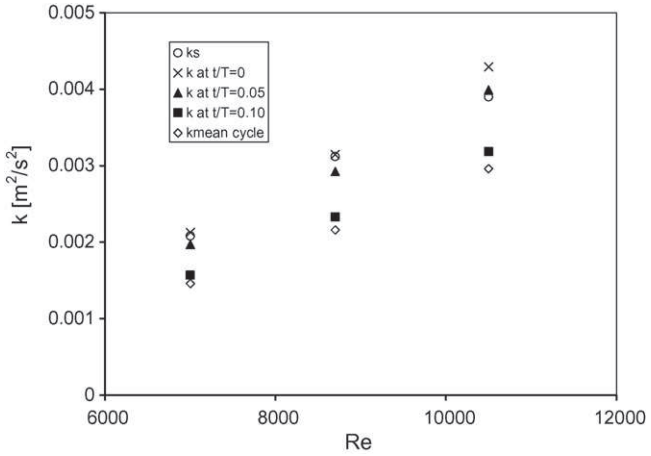

Fig. 8. Comparison of simulation results for k with its values k_s corresponding to experimental drop size at different Re number.

This study provides information for testing the second hypothesis, and the results are illustrated in Fig. 8. They are expressed as space-averaged value of k at different moments of the pulsation as a function of Re.

It is seen again that the total mean energy level (k mean cycle—space- and time-averaged value) performs worse results rather lower than the experimental data for d_s translated by the values of k_s. The stage mean energy at the moment of highest energy level ($t/T = 0$) corresponds quite well to k_s. However, a tendency for overestimation at higher Re numbers exists. At the moment $t/T = 0.05$ the coincidence with the experiment is also good and becomes better at higher Re. This is a positive tendency because higher Re numbers correspond to real practical situations. At the moment $t/T = 0.10$, which is the limit of high-energy period, the results become quite different from experimental ones.

Obviously the agreement with experimental results is improved when selecting over the periods of high energy. For the particular case, the choice of stage mean value at the moments of pulsation peaks as the characteristic value of turbulent kinetic energy is rather realistic. It seems that the development of more extended energy–drop size correlations for practical use should follow similar logic. This approach will be applied in a future study on the same type of equipment in order to obtain relations for the calculation of drop size based on energy level, which is useful for the determination of interphase contact surface.

6. Conclusion

Numerical hydrodynamic simulation of single-phase flow in a pulsed extraction column with internals of immobile discs and rings is carried out. The modeling is based on Reynolds equations coupled with k–ε model of turbulence. As far as pulsed flow is concerned, the evolution of turbulent kinetic energy k and its dissipation rate ε in the course of pulsation is thoroughly studied.

Pictures of spatial distribution of k and ε on the stage are obtained for different moments of a pulsation cycle, and zones with high-energy content and high-dissipation rate are spatially localized. It is found that they coincide with the sites of drop breakage.

Regarding the time evolution of energy, it is found that the stage energy during particular time periods of the pulsation cycle is significantly larger than the mean energy. A comparison with experimental data has shown that the mean (space- and time-averaged) energy of the pulsed flow does not represent adequately the real situation. A good approximation is found by using energy values during the recognized high-energy intervals of pulsation. It is to conclude that an "effective" energy level should be determined by selection over the high-energy time periods and zones in order to compensate the smoothing effect of mean energy level.

The results obtained are useful for the development of correlation for the calculation of drop size based on energy level at the stage, which is needed for the determination of parameters of practical interest, such as drop residence time and interphase mass transfer surface.

Appendix A. Nomenclature

A	amplitude of pulsation (m)
d	drop diameter (m)
d_s	maximal stable drop diameter (m)
D_c	column diameter (m)
D_d	disc diameter (m)
D_r	diameter of ring aperture (m)
E	roughness parameter, Eq. (3)
ΔE	difference of surface energy of mother and daughter drops, Eq. (7)
f	pulsation frequency (Hz)
F	free area of the plates (%)
H	interplate distance (m)
k	turbulent kinetic energy (m^2/s^2)
K	Karman constant
n	number of daughter drops
Re	Reynolds number, Eq. (2)
t	time (s)
T	period of pulsation (s)
U_m	mean flow velocity over a pulsation period (m/s)
U_o	permanent flow velocity (m/s)
$U_p(t)$	instantaneous velocity of the pulsed flow (m/s)
U_τ	friction velocity (m/s)
$U(y)$	velocity in logarithmic sublayer (m/s)
We	Weber number, Eq. (6)
y	distance from the wall (m)

Greek letters

δ	distance from the wall (m)
ε	dissipation rate of the turbulent kinetic energy (m^2/s^3)
ν	kinematic viscosity (m^2/s)
ρ_c	continuous phase density (kg/m^3)
σ	interfacial tension (N/m)

References

[1] Kirk-Othmer Encyclopedia of Chemical Technology, John Willey & Sons, NY, 1980.
[2] C. Hanson (Ed.), Recent Advances in Liquid–Liquid Extraction, Pergamon Press, Oxford, 1971.
[3] T.C. Lo, M.H.I. Baird, C. Hanson, Handbook of Solvent Extraction, John Wiley & Sons, NY, 1983.
[4] J.C. Godfrey, M.J. Slater (Eds.), Liquid–Liquid Extraction Equipment, John Wiley & Sons Ltd., NY, 1994.
[5] H. Tennekes, J.L. Lumley, A First Course of Turbulence, M.I.T. Press, Cambridge, MA, 1972.
[6] J.O. Hinze, Turbulence, McGraw Hill, London, 1975.
[7] G. Angelov, E. Journe, A. Line, C. Gourdon, Simulation of the flow patterns in a disc and doughnut column, Chem. Eng. J. 45 (1990) 87–97.
[8] M. Aoun, Numerical simulation of the hydrodynamics and axial mixing in pulsed discs-and-rings columns (Fr.), PhD thesis, INP Toulouse, 1995.
[9] G. Angelov, C. Gourdon, A. Line, Determination of turbulent flow energy characteristics in pulsed solvent extraction columns, in: Proc. I Europ. Congr. Chem. Eng., vol. 1, Florence, 1997, pp. 3021–3025.
[10] M. Aoun, P. Guiraud, CFD contribution to a design procedure for discs and doughnuts extraction columns, Chem. Eng. Res. Des. 76 (1998) 951–960.
[11] G. Angelov, C. Gourdon, A. Line, Simulation of flow hydrodynamics in a pulsed solvent extraction column under turbulent regimes, Chem. Eng. J. 71 (1998) 1–9.
[12] C. Berner, F. Durst, D.M. McEligot, Flow around baffles, J. Heat Transfer 106 (1984) 743–749.
[13] W.Z. Oh, Hydrodynamic study of a pulsed column with discs and rings (Fr.), PhD thesis, INP Toulouse, 1983.
[14] L. Boyadzhiev, M. Spassov, On the size of drops in pulsed and vibrating plate extraction columns, Chem. Eng. Sci. 37 (2) (1982) 337–340.
[15] M.F. Buratti, Study on the axial mixing in pulsed columns with internals of discs and doughnuts (Fr.), PhD thesis, INP Lorraine, 1988.
[16] A. Laulan, Hydrodynamics and drop break-up in a pulsed disc and ring column (Fr.), PhD thesis, INP Toulouse, 1980.
[17] S.W. Tu, B.R. Ramaprian, Fully developed period turbulent pipe flow: experimental results and comparison with predictions, J. Fluid Mech. 133 (1983) 31–58.
[18] W. Rodi, Turbulence Models for Practical Applications, Von Karman Institute of Fluid Dynamics, Germany, 1985.
[19] B.E. Launder, D.B. Spalding, Mathematical Models of Turbulence, Academic Press, London, 1972.
[20] G. Angelov, C. Gourdon, Estimation of boundary conditions for the simulation of turbulent flow in stagewise extraction columns, Hung. J. Ind. Chem. 25 (1997) 223–228.
[21] J.M. Bujalski, W. Yang, J. Nikolov, C.B. Solnordal, M.P. Schwarz, Measurement and CFD simulation of single-phase flow in solvent extraction pulsed column, Chem. Eng. Sci. 61 (2005) 2930–2938.
[22] S. Retieb, Eulerian simulations of two-phase liquid–liquid and solid–liquid contactors (Fr.), PhD thesis, INP Toulouse, 1999.
[23] S. Retieb, P. Guiraud, G. Angelov, C. Gourdon, Hold-up within two-phase countercurrent pulsed column via Eulerian simulations, Chem. Eng. Sci. 62 (17) (2007) 4558–4572.
[24] R. Schiestel, Modeling and Simulation Of Turbulent Flows (Fr.), Hermes, Paris, 1993.
[25] G. Narsimhan, J.P. Gupta, D. Ramkrishna, A model for transitional breakage probability of droplets in agitated liquid–liquid dispersions, Chem. Eng. Sci. 34 (1979) 257–265.
[26] N. Bardin-Monnier, P. Guiraud, C. Gourdon, Residence time distribution of droplets within discs and doughnuts pulsed extraction columns via Lagrangian experiments and simulations, Chem. Eng. J. 94 (3) (2003) 241–254.